THE JOURNAL OF BIOLOGICAL CHEMISTRY
Vol. 277, No. 28, Issue of July 12, pp. 25152–25159, 2002

Printed in U.S.A.

Marked Perinatal Lethality and Cellular Signaling Deficits in Mice Null for the Two Sphingosine 1-Phosphate (S1P) Receptors, $S1P_2/LP_{B2}$/EDG-5 and $S1P_3/LP_{B3}$/EDG-3*

Received for publication, January 7, 2002, and in revised form, April 30, 2002
Published, JBC Papers in Press, May 2, 2002, DOI 10.1074/jbc.M200137200

Isao Ishii‡§, Xiaoqin Ye‡, Beth Friedman‡, Shuji Kawamura‡, James J. A. Contos‡, Marcy A. Kingsbury‡, Amy H. Yang¶, Guangfa Zhang‡, Joan Heller Brown‡¶, and Jerold Chun‡¶‖

From the ‡Department of Pharmacology and the ¶Neurosciences and Biomedical Sciences Programs, School of Medicine, University of California at San Diego, La Jolla, California 92093-0636 and the §Department of Molecular Genetics, National Institute of Neuroscience, National Center of Neurology and Psychiatry (NCNP), Ogawahigashi 4-1-1, Kodaira, Tokyo 187-8502, Japan

Five cognate G protein-coupled receptors ($S1P_{1–5}$) have been shown to mediate various cellular effects of sphingosine 1-phosphate (S1P). Here we report the generation of mice null for $S1P_2$ and for both $S1P_2$ and $S1P_3$. $S1P_2$-null mice were viable and fertile and developed normally. The litter sizes from $S1P_2S1P_3$ double-null crosses were remarkably reduced compared with controls, and double-null pups often did not survive through infancy, although double-null survivors lacked any obvious phenotype. Mouse embryonic fibroblasts (MEFs) were examined for the effects of receptor deletions on S1P signaling pathways. Wild-type MEFs were responsive to S1P in activation of Rho and phospholipase C (PLC), intracellular calcium mobilization, and inhibition of forskolin-activated adenylyl cyclase. $S1P_2$-null MEFs showed a significant decrease in Rho activation, but no effect on PLC activation, calcium mobilization, or adenylyl cyclase inhibition. Double-null MEFs displayed a complete loss of Rho activation and a significant decrease in PLC activation and calcium mobilization, with no effect on adenylyl cyclase inhibition. These data extend our previous findings on $S1P_3$-null mice and indicate preferential coupling of the $S1P_2$ and $S1P_3$ receptors to Rho and PLC/Ca^{2+} pathways, respectively. Although either receptor subtype supports embryonic development, deletion of both produces marked perinatal lethality, demonstrating an essential role for combined S1P signaling by these receptors.

Sphingosine 1-phosphate (S1P)[1] is a bioactive lysophospholipid that elicits diverse physiological effects on most types of cells and tissues. Several lines of evidence from a wealth of *in vitro* studies revealed that these effects are induced by S1P activation of any of five cognate G protein-coupled receptors: $S1P_1$ (LP_{B1}/EDG-1), $S1P_2$ (LP_{B2}/H218/AGR16/EDG-5), $S1P_3$ (LP_{B3}/EDG-3), $S1P_4$ (LP_{C1}/EDG-6), and $S1P_5$ (LP_{B4}/NRG-1/EDG-8) (reviewed in Refs. 1–7). In part reflecting a lack of receptor subtype-specific agonists/antagonists and the universal expression of multiple S1P receptor genes in many single cell types, the *in vivo* roles of each receptor were unclear until the recent use of genetic approaches in mice (reviewed in Ref. 44).

Liu *et al.* (8) reported that $S1P_1$-null mice are lethal. $S1P_1$-null mice exhibit embryonic hemorrhage and incomplete vascular maturation, which lead to intrauterine death. S1P-induced cell migration and activation of the small GTPase Rac are severely defective in $S1P_1$-null mouse embryonic fibroblasts (MEFs), suggesting that the loss of S1P cellular signaling is relevant to those phenotypes found in $S1P_1$-null mice (8). We observed that $S1P_3$-null mice are without marked phenotypic differences compared with controls (9). However, S1P-induced phospholipase C (PLC) activation is severely defective in $S1P_3$-null MEFs (9). In this study, we generated $S1P_2$-null mice. $S1P_2$-null mice were viable and apparently normal, as were $S1P_3$-null mice. However, S1P-induced Rho activation was impaired. By contrast, PLC activation, intracellular calcium mobilization, and adenylyl cyclase inhibition were normal in $S1P_2$-null MEFs.

To determine whether the $S1P_2$ and $S1P_3$ receptors serve redundant functions, we further generated mice null for these two receptor subtypes, $S1P_2S1P_3$ double-null mice. A remarkable *in vivo* phenotype was found in double-null mice: markedly decreased litter sizes from double-null crosses. In addition, *in vitro* analysis of receptor function demonstrated that S1P-induced activation of Rho and PLC and intracellular calcium mobilization, but not adenylyl cyclase inhibition, were severely defective in double-null MEFs. These results identify a new physiological function for S1P receptor signaling and perinatal survival and indicate non-redundant signaling roles for these individual lysophospholipid receptors.

EXPERIMENTAL PROCEDURES

Materials—[α-^{32}P]dCTP and *myo*-[2-^{3}H]inositol were purchased from Perkin-Elmer Life Sciences. S1P and lysophosphatidic acid (LPA; 1-oleoyl-2-hydroxy-*sn*-glycero-3-phosphate) were purchased from Avanti Polar Lipids (Alabaster, AL). Pertussis toxin (PTX) and Fura 2/AM were purchased from Calbiochem and Wako Pure Chemical Industries (Osaka, Japan). Rhotekin Rho-binding domain- and PAK1 p21-binding domain-conjugated agarose beads were both purchased from Upstate

* This work was supported by an unrestricted gift from Merck Research Laboratories (to J. C.); National Institute of Mental Health Grant R01 MH51699 (to J. C.); a grant from the Mitsubishi Pharma Research Foundation (to I. I.); National Science Foundation Grant 00747776 (to B. F.); National Institutes of Health Grants GM36927 and HL28143 (to S. K. and J. H. B.), Neuroplasticity of Aging Training Grant 5T32AG00216 (to M. A. K.), and NIGMS Pharmacology Training Grant 2T32GM07752 (to A. H. Y.); and a grant from the National Institute of Neuroscience, NCNP, Japan (to Dr. Hideo Kimura). The costs of publication of this article were defrayed in part by the payment of page charges. This article must therefore be hereby marked "*advertisement*" in accordance with 18 U.S.C. Section 1734 solely to indicate this fact.

‖ To whom correspondence should be addressed: Merck Research Laboratories, San Diego, 3535 General Atomics Ct., San Diego, CA 92121. Tel.: 858-202-5232; Fax: 858-202-5813; E-mail: jerold_chun@merck.com.

[1] The abbreviations used are: S1P, sphingosine 1-phosphate; MEF, mouse embryonic fibroblast; PLC, phospholipase C; LPA, lysophosphatidic acid; PTX, pertussis toxin; PAK, p21-activated kinase; ORF, open reading frame; BSA, bovine serum albumin.

Biotechnology, Inc. (Lake Placid, NY). The pMC1DT-3 vector (10) was a kind gift from Dr. Takeshi Yagi (National Institute for Physiological Sciences, Okazaki, Japan). The pFlox vector (11) and R1 embryonic stem cells were generous gifts from Dr. Jamey D. Marth (University of California at San Diego). Trizol and all cell culture reagents were purchased from Invitrogen. Forskolin, 3-isobutyl-1-methylxanthine, and other reagents were purchased from Sigma, unless otherwise noted. Mice (C57BL/6NCrlBr) were purchased from Charles River Laboratories (Wilmington, MA).

Generation of s1p$_2$ Mutant Mice—The isolation of an *s1p$_2$* λ clone from a 129/SvJ mouse genomic DNA library (Stratagene, La Jolla, CA) was described previously (12). The 1.7-kb *PGKneo* gene (a *Nhe*I/*Bam*HI fragment of the pFlox vector (11)), the 6.5-kb long arm (a *Bgl*II/*Xho*I fragment upstream of the open reading frame (ORF)), and the 1.0-kb short arm (a *Not*I/*Xba*I fragment downstream of the ORF) were subcloned successively into the pBluescript SK(+) vector (Stratagene). Then, the *Not*I/*Xho*I fragment of the vector was cloned into the *Not*I/*Xho*I sites of the pMC1DT-3 vectors, producing the *s1p$_2$* targeting vector used in this study. The *Not*I-linearized targeting construct was electroporated into R1 embryonic stem cells using Gene-Pulser II (Bio-Rad). The targeting was completed by homologous recombination under G418 (200 μg/ml) positive selection and diphtheria toxin A subunit-catalyzed negative selection, which produced a recombinant knockout allele in embryonic stem cells. A hemizygous embryonic stem clone was injected into C57BL/6N blastocysts to produce chimeric male mice, which were then crossed with C57BL/6N females to obtain *agouti s1p$_2$*-heterozygous pups. All mice analyzed were obtained from intercrosses between their progenies, *s1p$_3$*-heterozygous or -homozygous (9), and C57BL/6N mice.

Care and Genotyping of Mice—Mice were housed in an air-conditioned room kept on a 12-h dark/light cycle and fed standard dry rodent food pellets *ad libitum*. The *s1p$_2$* genotyping was done by Southern blot analysis and, more routinely, by PCR using tail genomic DNA and the following three primer sets: primer 1, 5′-ACACCCTTTGTATCAAGTGGCAA-3′; primer 2, 5′-TTCTGGAGGGTAACACAGTGGT-3′; and primer 3, 5′-GCTAAAGCGCATGCTCCAGACT-3′. The PCR conditions were 35 cycles of 94 °C for 30 s, 56 °C for 1 min, and 72 °C for 1 min.

Northern Blot Analysis—Mouse tissues were quickly removed and homogenized in the Trizol reagent with the Tissue Tearor (Biospec Products, Inc., Bartlesville, OK). Total RNA was isolated following the instructions of Invitrogen, and 20 μg of each RNA was analyzed as described previously (9, 13). Specific probes used were the ORF sequences for the mouse *lpa$_1$*, *s1p$_{1–3}$*, and *s1p$_5$* genes and *s1p$_4$* cDNA (9).

Histological Analysis—Histological analyses for *s1p$_2$* phenotypes were done on the progenies on a purer C57BL/6N background (backcrossed three to five generations; N3–N5). The *s1p$_2$*-heterozygous (*s1p$_2^{+/-}$*) males and females (N3–N5) were bred to obtain all three genotypes, wild-type (*s1p$_2^{+/+}$*), heterozygous (*s1p$_2^{+/-}$*), and homozygous (*s1p$_2^{-/-}$*), within the litters. For S1P$_2$S1P$_3$ double-null analysis, *s1p$_2^{+/-}$s1p$_3^{-/-}$* males and females on mixed backgrounds of 129/SvJ and C57BL/6N were bred to obtain three genotypes, *s1p$_2^{+/+}$s1p$_3^{-/-}$*, *s1p$_2^{+/-}$s1p$_3^{-/-}$*, and *s1p$_2^{-/-}$s1p$_3^{-/-}$*, within the litters. In both analyses, these littermates were compared at three developmental stages (10 days and 4 and 8 weeks) as described previously (9). The mice were anesthetized with Nembutal sodium solution (0.75 mg/g of body weight; Abbott). Anesthetized mice were perfused through the heart with 0.9% NaCl, followed by 4% paraformaldehyde in phosphate-buffered saline. Each tissue (except brain) was dissected out, post-fixed overnight in 4% paraformaldehyde in phosphate-buffered saline at 4 °C, and processed for paraffin embedding. Five-μm sections were cut, processed, and stained with hematoxylin and eosin according to standard protocols. For brain analysis, whole brain was dissected out, post-fixed as described above, cryoprotected in 30% sucrose, and sectioned on a cryostat. Twenty-μm sections were cut and then stained with cresyl violet according to standard protocols.

Preparation of MEFs—MEFs were prepared from embryonic day 14 embryos generated by the wild-type or knockout (single or double) intercrosses as described previously (9). MEFs were maintained as a monolayer culture on tissue culture dishes in Dulbecco's modified Eagle's medium supplemented with 10% heat-inactivated fetal bovine serum and antibiotics. Cells from the second to third passages were used for analyses.

Functional Assays in MEFs—All functional assays except for the intracellular calcium mobilization assay were carried out as described previously (9). Briefly, for the PLC assay, MEFs on 12-well dishes were prelabeled with [^{3}H]inositol (2 μCi/well) in inositol- and serum-free medium for 24 h and stimulated with S1P or LPA in Hepes/Tyrode's/BSA buffer (14). After a 20-min incubation, radioactivity in the inositol monophosphate + inositol bisphosphate + inositol trisphosphate fractions of the cell extracts was examined as described previously (9, 13, 14). The activity was expressed as a percentage of the 10 μM LPA-induced response.

For cAMP determination, MEFs on 24-well dishes were preincubated in Hepes/Tyrode's/BSA buffer containing 0.5 mM 3-isobutyl-1-methylxanthine for 20 min and then stimulated for 20 min with or without 1 μM forskolin in the presence or absence of S1P. cAMP contents were measured with the cAMP enzyme immunoassay system (Amersham Biosciences) following the manufacturer's instructions. The activity was expressed as percentages of basal levels or 1 μM forskolin-induced cAMP accumulation.

For Rho and Rac assays (9), MEFs on 10-cm dishes were incubated for 10 min in Hepes/Tyrode's/BSA buffer and then stimulated for 3 min with S1P or LPA. Cells were lysed and incubated with Rhotekin Rho-binding domain- and PAK1 p21-binding domain-conjugated agarose beads, respectively. GTP-bound active forms of Rho or Rac protein were specifically detected by Western blot analysis using anti-RhoA (Santa Cruz Biotechnology, Inc., Santa Cruz, CA) and anti-Rac1 (BD PharMingen) antibodies, respectively. Rho protein in 5% of the cell lysate and Rac protein in 1% of the cell lysate were also detected as references, respectively.

For calcium mobilization assay, MEF cells were loaded with Fura 2/AM (1 μM) in Hepes/Tyrode's/BSA buffer for 1 h. The cells were successively stimulated with 10 μM S1P, 10 μM LPA, and 1 mM ATP in Hepes/Tyrode's/BSA buffer containing 1.8 mM $CaCl_2$. Measurements of intracellular calcium concentration were performed using a Hitachi F-2000 fluorescence spectrophotometer at excitation wavelengths of 340 and 380 nm and an emission wavelength of 510 nm. Conversion of the 340/380 nm ratio value into nanomolar intracellular Ca^{2+} was estimated by comparing the cellular fluorescence ratio with ratios acquired with buffers containing known Ca^{2+} concentrations.

Data Representation—Data are the means ± S.E. of triplicate samples from a single experiment representative of two to three experiments that gave similar results. Statistical analyses were done by Student's t test or the χ^2 test (in tables), and a difference of $p < 0.01$ was considered to be statistically significant.

RESULTS

Generation of S1P$_2$-null Mice—The genomic structure of *s1p$_2$* consists of two exons, with the entire ORF encoded in the second exon (12). Therefore, the entire ORF was deleted in R1 embryonic stem cells by replacing it with a neomycin-resistance gene (Fig. 1*A*). The correct integration of the targeting construct was confirmed by Southern blot analysis using probes both inside (*Probe B*) and outside (*Probe A*) of the ORF (Fig. 1, *A* and *B*, *left panels*). A single correctly targeted embryonic stem clone was injected into blastocysts, and a series of mice with mutated *s1p$_2$* alleles (*s1p$_2^{+/-}$* or *s1p$_2^{-/-}$*) were established. Mice genotypes were confirmed by Southern blot (Fig. 1*B*, *right panel*) or PCR (Fig. 1*C*) analysis using tail genomic DNA. The complete absence of *s1p$_2$* transcripts in *s1p$_2^{-/-}$* mice was confirmed by Northern blot analysis of adult tissues in which *s1p$_2$* is normally expressed at high levels (9): heart, brain, lung, and spleen (Fig. 1*D*, *left panel*). Moderate levels of *s1p$_2$* expression were observed in *s1p$_2^{+/-}$* tissues (Fig. 1*D*, *left panel*). In those tissues, several other S1P receptor genes (*s1p$_1$* and *s1p$_{3–5}$*) and an LPA receptor gene (*lpa$_1$*) were also expressed. There were no significant changes in the expression levels of those genes related to *s1p$_2$* deficiency.

No Obvious Phenotypic Abnormality in S1P$_2$-null Mice—S1P$_2$-null mice were generally obtained with the expected mendelian frequency and without sexual bias (Table I). S1P$_2$-null mating produced S1P$_2$-null pups, although the average litter size was modestly but significantly ($p < 0.01$) smaller than that from *s1p$_2^{+/-}$* males × wild-type females (6.5 *versus* 8.6 pups/litter). The average size from *s1p$_2^{+/-}$* males × *s1p$_2^{-/-}$* females (6.7 pups/litter) was smaller than that from *s1p$_2^{+/-}$* males × wild-type females (8.6 pups/litter) or from *s1p$_2^{-/-}$* males × *s1p$_2^{+/-}$* females (8.1 pups/litter) (Table I), suggesting possible defects in *s1p$_2^{-/-}$* females, but not in *s1p$_2^{-/-}$* males.

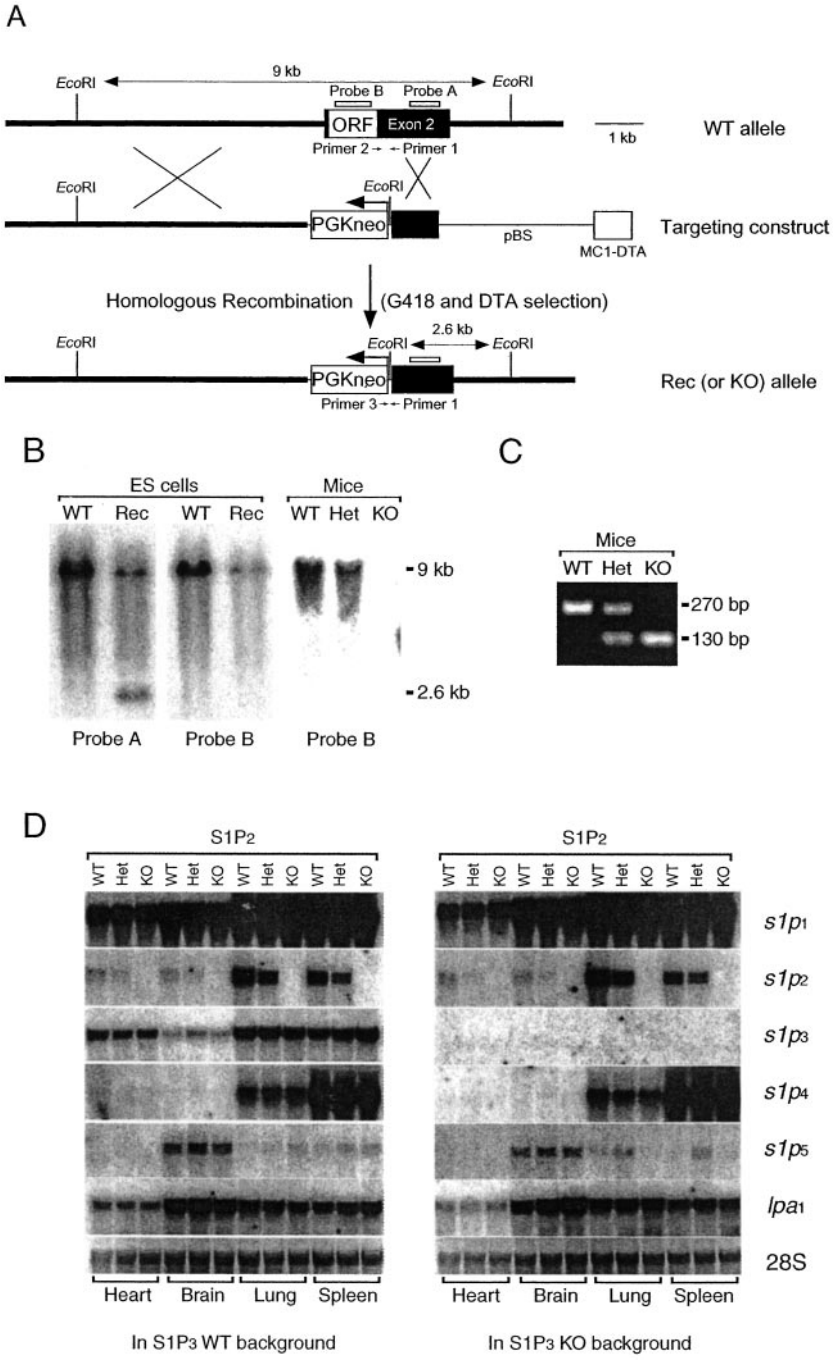

FIG. 1. **Generation of S1P$_2$-null and S1P$_2$S1P$_3$ double-null mice.** *A*, *s1p$_2$* gene targeting. The structures of the wild-type (*WT*) allele, targeting construct, and recombinant (*Rec*; or knockout (*KO*)) allele are shown. The *s1p$_2$* ORF was replaced with the neomycin-resistance gene (*neo*) driven by the phosphoglycerate kinase (*PGK*) promoter. The Southern blot probes (*Probes A* and *B*) and the sizes of the restriction enzyme (*Eco*RI) fragments detected with those probes are indicated. Approximate positions of PCR primers used for genotyping are also shown. *DTA*, diphtheria toxin A. *B*, Southern blot analysis of *Eco*RI-digested genomic DNA from properly targeted R1 embryonic stem (*ES*) cell clones and mutants generated by crossing *s1p$_2$*-heterozygous (*Het*) mice. *C*, PCR genotyping for *s1p$_2$* (PCR product sizes of 270 and 130 bp, respectively). *D*, Northern blot analysis of RNAs from heart, brain, lung, and spleen isolated from adult male wild-type, *s1p$_2$*-heterozygous, and *s1p$_2$*-knockout littermates on an *s1p$_3$*-wild-type (*left panel*) or *s1p$_3$*-knockout (*right panel*) background. The probes used are indicated. Ribosomal 28 S RNA stained with ethidium bromide is shown as a loading control.

TABLE I
Inheritance of the s1p$_2$ mutant allele

Total litter numbers, average litter sizes (means ± S.D.), and numbers of genotyped offsprings from the indicated crosses are shown. WT, wild-type; Het, heterozygous; KO, knockout.

Parental genotypes	Total litter no.	Average litter sizes	Offspring genotypes at weaning ages (~3 weeks)								
			Males			Females			Both sexes		
Male × Female			WT	Het	KO	WT	Het	KO	WT	Het	KO
Het × WT	20	8.6 ± 2.6	42	48		46	36		88	84	
Het × Het	56	7.8 ± 2.5	57	100	56	56	124	44	113	224	100
Het × KO	24	6.7 ± 2.3		42	42		39	37		81	79
KO × Het	19	8.1 ± 2.3		43	38		29	44		72	82
KO × KO	22	6.5 ± 2.1			73			69			142

S1P$_2$-null mice did not differ from the wild-type or *s1p$_2^{+/-}$* littermates in gross appearance, general behavior, overall health, and longevity (through at least 20 months). There were no significant differences in body weights among *s1p$_2$* genotypes in littermates at 4 or 8 weeks of age in each sex (data not shown). Routine histology was performed in major tissues (brain, heart, lung, thymus, liver, kidney, spleen, adipose tissues, skin, muscle, stomach, intestine, uterus, and testis) from

mice at 10 days and 4 and 8 weeks of age and revealed no obvious differences among $s1p_2$ genotypes in littermates of either sex (data not shown). Also, routine hematology, including erythrocyte, leukocyte, and platelet counts; neutrophil, lymphocyte, monocyte, and eosinophil proportions; glucose, cholesterol, and triglyceride serum levels; and lipase activity (9), failed to detect any abnormality or difference in $S1P_2$-null *versus* wild-type mice (data not shown).

Generation and Analysis of $S1P_2S1P_3$ Double-null Mice—The viability and fertility of both $S1P_2$-null and $S1P_3$-null mice (9) enabled the generation of $S1P_2S1P_3$ double-null mice by successive crossbreeding. First, $s1p_2^{+/-}s1p_3^{+/-}$ double-heterozygous mice were produced from any of the following crosses: $s1p_2^{-/-}$ males × $s1p_3^{-/-}$ females, $s1p_3^{-/-}$ males × $s1p_2^{-/-}$ females, $s1p_2^{-/-}s1p_3^{-/-}$ males × wild-type females, and wild-type males × $s1p_2^{-/-}s1p_3^{-/-}$ females, which gave averages of 5.8–7.0 pups/litter (Table II). Next, $s1p_2^{+/-}s1p_3^{+/-}$ mice were bred to produce 12 $s1p_2^{-/-}s1p_3^{-/-}$ mice (eight males and four females). The breeding produced several $s1p_2^{+/-}s1p_3^{-/-}$ or $s1p_2^{-/-}s1p_3^{+/-}$ mice, which were also used to produce double-null mice (Table II). The most striking phenotype of the double-null mice was revealed in the vastly reduced number of progeny obtained by crossing double-null mice, far less than expected based on the mendelian frequency (Table II).

$S1P_2S1P_3$ double-null mice from $s1p_2^{+/-}s1p_3^{-/-}$ intercrosses were analyzed with their $S1P_3$-null littermates as controls because our previous studies did not reveal any major phenotypic abnormality in $S1P_3$-null mice (9). The complete absence of $s1p_2$ and $s1p_3$ transcripts in double-null mice was confirmed by Northern blot analysis of RNA samples from heart, brain, lung, and spleen (Fig. 1*D*, *right panel*). There was no obvious compensatory gene expression of other S1P receptors (Fig. 1*D*, *right panel*). Double-null mice did not differ from their $S1P_3$-null littermates in gross appearance, general behavior, overall health, body weight, and longevity (through at least 16 months) (data not shown). Routine histology and hematology did not reveal any gross differences related to $S1P_2$ deficiency on the $s1p_3^{-/-}$ background (data not shown). However, double-null pups generated by double-null mating were lost perinatally at high frequency. Among 65 neonates (including carcasses) produced from 21 pregnancies, 39 neonates were found dead within 1 week after birth (most died within 24 h); the remaining 26 neonates survived to adulthood. Maternal negligence of pups was observed in most of the 13 pregnancies with no neonatal survivors, a phenomenon rarely observed in the other crosses. Among eight pregnancies that had survivors, one pregnancy had six survivors, two had four each, three had three each, one had two, and one had one (total of 26 mice). Unexpectedly, the neonatal survivors grew up normally and did not show any obvious abnormality with maturation.

Expression of S1P Receptor Genes in MEF Cells—To determine the contribution of $s1p_2$ (and/or $s1p_3$) deletion to S1P cellular signaling, we analyzed MEF cells prepared from embryonic day 14 embryos. First, expression of the *s1p* genes in each cell preparation was examined by Northern blot analysis (Fig. 2). Consistent with our previous observation (9), wild-type MEF cells expressed $s1p_{1-3}$, but neither $s1p_4$ nor $s1p_5$. As expected, MEF cells from each of the mutants lacked expression of their corresponding *s1p* gene(s). There were no obvious compensatory changes in the expression of other S1P receptor genes or an LPA receptor gene, lpa_1 (Fig. 2).

S1P-induced PLC Activation in MEF Cells—S1P concentration-dependent PLC activation was measured using radioisotope labeling methods (see "Experimental Procedures"). MEF cells express two LPA receptor genes (lpa_1 and lpa_2) and were responsive to LPA in both PLC and Rho activation (13).[2] The responses to LPA stimulation were comparable among the MEF cell types (4.3–6.0-fold induction above basal levels at 10 μM), and thus, S1P-induced responses were expressed as a percentage of the 10 μM LPA-induced response.

As observed previously (9), wild-type MEF cells were highly responsive to S1P in PLC activation, whereas $S1P_3$-null cells showed markedly diminished PLC activation in response to S1P (Fig. 3). Deletion of the $S1P_2$ receptor did not affect this response because S1P-induced PLC activation in $S1P_2$-null cells was comparable to that in wild-type cells, and that in $S1P_2S1P_3$ double-null cells was comparable to that in $S1P_3$-null cells (Fig. 3). These results indicate that the $S1P_2$ receptor does not mediate PLC activation in response to S1P in these cells. This is consistent with our previous observation that $s1p_2$ overexpression does not affect S1P-induced PLC activation in $S1P_3$-null MEF cells (9).

S1P-induced Intracellular Calcium Mobilization in MEF Cells—S1P-induced intracellular calcium mobilization was measured by Fura 2/AM labeling methods (see "Experimental Procedures"). Wild-type MEF cells were highly responsive to both S1P and LPA (Fig. 4*A*). Deletion of $S1P_3$, but not $S1P_2$, in MEF cells resulted in no or minimal response to S1P in calcium mobilization, whereas responses to LPA or ATP were comparable among all MEF cell types (Fig. 4, *B–D*). These results indicate that $S1P_3$, but not $S1P_2$, plays a major role in S1P-induced intracellular calcium mobilization.

S1P-induced Modulation of Adenylyl Cyclase Activity in MEF Cells—First, we compared the effects of S1P on forskolin-induced cAMP accumulation in each of the mutant MEF cells. The concentration-dependent inhibitory effects of S1P were comparable among wild-type, $S1P_2$-null, and $S1P_2S1P_3$ double-null cells (Fig. 5*A*), indicating negligible contributions of either $S1P_2$ or $S1P_3$ to the adenylyl cyclase inhibitory actions of S1P. The inhibitory curve obtained with $S1P_3$-null mice was slightly shifted rightward, as observed previously (9). Next, we examined the effects of S1P on the basal cAMP levels in PTX-treated and PTX-untreated cells (Fig. 5*B*). S1P did not affect the basal cAMP levels in PTX-untreated wild-type cells, as observed previously (9); however, it significantly increased the basal cAMP levels in PTX-treated cells (Fig. 5*B*, *upper left panel*). In contrast, S1P significantly decreased the basal cAMP levels in untreated $S1P_2S1P_3$ double-null cells, whereas it did not affect those in PTX-treated double-null cells (Fig. 5*B*, *lower right panel*). Both of the S1P actions (stimulatory and inhibitory) on either $S1P_2$-null or $S1P_3$-null cells seemed to be in between those on wild-type and double-null cells (Fig. 5*B*, *upper right* and *lower left panels*).

S1P-induced Rho Activation in MEF Cells—S1P-induced activation of Rho or Rac was examined using activated Rho or Rac pull-down assays (Fig. 6). S1P activated Rho in wild-type and $S1P_3$-null cells in a similar fashion (Fig. 6*A*), as observed previously (9). In contrast, S1P activated Rho to a much lesser extent in $S1P_2$-null cells. Interestingly, S1P failed to activate Rho in double-null cells (Fig. 6*A*). LPA activated Rho similarly in all of the mutant MEF cells (Fig. 6*B*), indicating that the lipid-receptor-Rho coupling was not generally impaired in the mutant MEF cells. These results indicate both major roles of $S1P_2$ and minor roles of $S1P_3$ in S1P-induced Rho activation in MEF cells. S1P did not induce Rac activation in any of the MEF cell types (Fig. 6*C*).

[2] J. J. A. Contos, I. Ishii, N. Fukushima, M. A. Kingsbury, X. Ye, and J. Chun, submitted for publication.

TABLE II
Inheritance of the s1p$_2$ and s1p$_3$ mutant alleles
Total litter numbers, average litter sizes (means ± S.D.), and numbers of genotyped offspring from the indicated crosses are shown. WT, wild-type; Het, heterozygous; KO, knockout.

Parental genotypes						Total litter no.	Average litter sizes	Offspring genotypes at weaning ages (~3 weeks)								Sex ratio (female/male)
Male			Female					*s1p$_2$*-WT			*s1p$_2$*-Het		*s1p$_2$*-KO			
s1p$_2$		*s1p$_3$*	*s1p$_2$*		*s1p$_3$*			*s1p$_3$*-WT	*s1p$_3$*-Het	*s1p$_3$*-KO	*s1p$_3$*-WT	*s1p$_3$*-Het	*s1p$_3$*-WT	*s1p$_3$*-Het	*s1p$_3$*-KO	
Het	×	WT	WT	×	WT	20	8.6 ± 2.6	88		84						82:90
WT	×	Het	WT	×	WT	18	7.5 ± 2.7	74	61							59:76
KO	×	WT	WT	×	KO	22	7.0 ± 2.6				153					72:81
WT	×	KO	KO	×	WT	23	6.7 ± 2.2				153					69:84
KO	×	KO	WT	×	WT	24	6.7 ± 3.0				161					88:73
WT	×	WT	KO	×	KO	15	5.8 ± 2.4				87					36:51
Het	×	Het	Het	×	Het	73	5.8 ± 2.8	34	48	32	62	116	59	22	38	12	193:230
Het	×	KO	Het	×	Het	21	5.2 ± 2.8		17	16		36	21		13	5	43:65
KO	×	Het	Het	×	Het	16	5.8 ± 2.5				16	24	12	16	15	10	46:47
Het	×	KO	Het	×	KO	47	4.6 ± 2.3			55			126			34	105:110
KO	×	Het	KO	×	Het	13	3.9 ± 1.6							14	31	6	23:28
KO	×	KO	Het	×	Het	8	5.6 ± 3.9					14	13		11	10	20:28
KO	×	KO	KO	×	Het	8	4.1 ± 1.8								19	13	18:14
KO	×	KO	KO	×	KO	21	1.2 ± 1.8									26	13:13

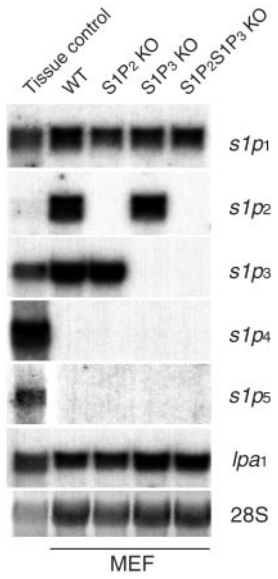

FIG. 2. **Expression of S1P receptor genes in wild-type, S1P$_2$-null, S1P$_3$-null, and S1P$_2$S1P$_3$ double-null MEF cells.** MEF cell RNAs prepared from wild-type (*WT*) and knockout (*KO*) embryonic day 14 embryos were analyzed by Northern blot analysis. Tissue RNA isolated from an adult C57BL/6N female was used as a positive control (heart RNA for *s1p$_{1-3}$*, lung RNA for *s1p$_4$*, and brain RNA for *s1p$_5$*). As loading control, ribosomal 28 S RNA was stained with ethidium bromide.

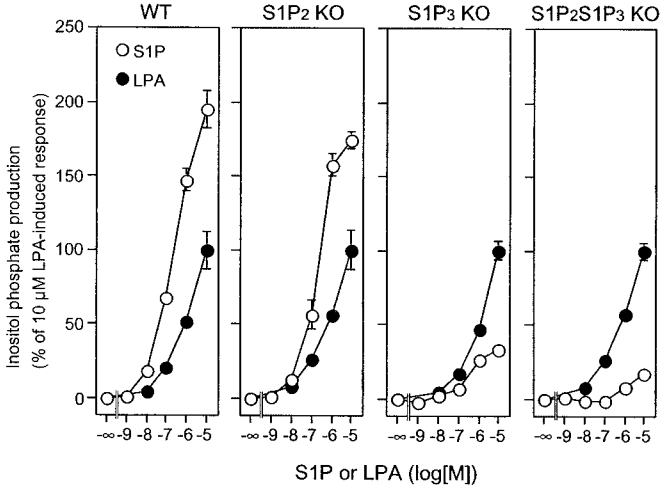

FIG. 3. **S1P-induced inositol phosphate production in MEF cells.** MEF cells (wild-type (*WT*) and each mutant) prelabeled with [^{3}H]inositol were stimulated with various concentrations of S1P or LPA for 20 min, and the radioactivity in the inositol phosphate fraction of the cell extract was determined. The activity is expressed as a percent response compared with 10 μM LPA as 100%. The responses to LPA were comparable in all of the MEF cells (4.3–6.0-fold induction above basal levels). Data shown are the means ± S.E. of triplicate samples. *Error bars* are not shown when the bars are smaller than the size of the *data points*. *KO*, knockout.

DISCUSSION

The existence of multiple S1P receptors with different functions in native cells underlies a variety of cellular responses elicited by S1P. Among five cognate mammalian S1P receptor genes, the expression of *s1p$_{1-3}$* is widespread throughout the mouse body, whereas that of *s1p$_4$* and *s1p$_5$* is more restricted (9, 12, 15, 16). It has been shown that many primary cell types such as MEFs (8, 9), atrial and ventricular myocytes (17), aortic smooth muscle cells (18), aortic endothelial cells (19, 20), and umbilical vein endothelial cells (20) express *s1p$_{1-3}$*. Thus, it is likely that these three receptors are the primary *in vivo* targets

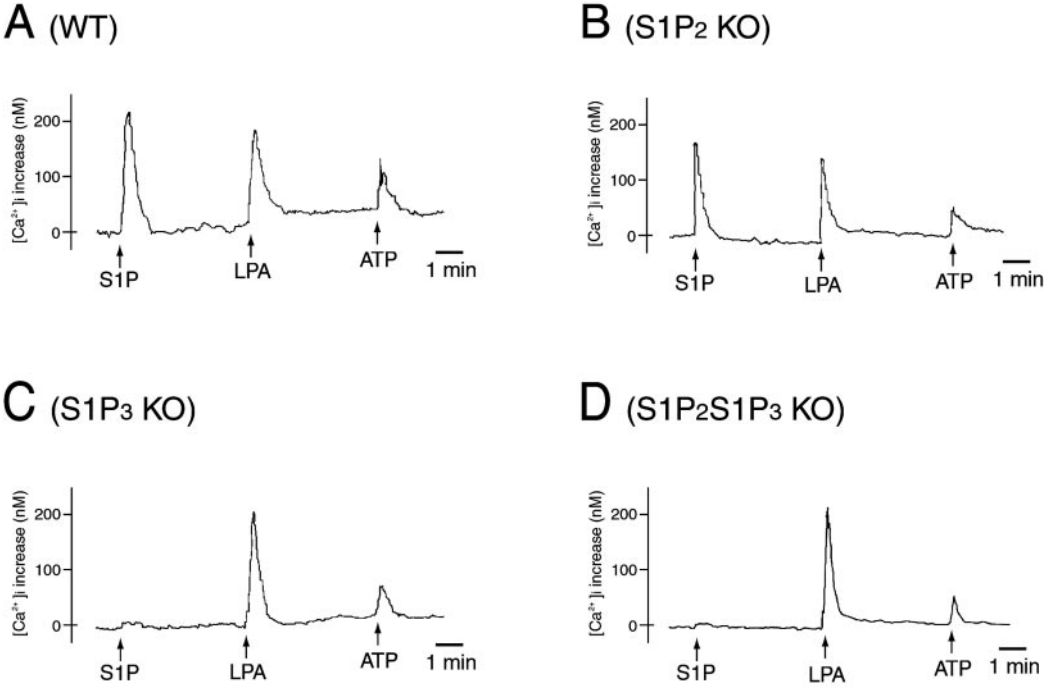

FIG. 4. **S1P-induced intracellular calcium mobilization in MEF cells.** MEF cells (wild-type (*WT*) and each mutant) were loaded with Fura 2/AM and stimulated successively with 10 μM S1P, 10 μM LPA, and 1 mM ATP. The increases in nanomolar intracellular Ca^{2+} ($[Ca^{2+}]_i$) from the basal levels (≅150 nM) are shown. Data are representative of three independent experiments. *KO*, knockout.

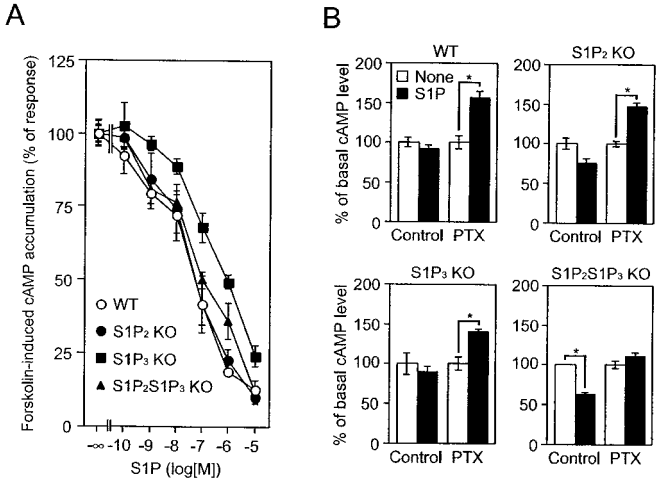

FIG. 5. **S1P-induced modulation of adenylyl cyclase activity in MEF cells.** Intracellular cAMP content after 20-min stimulation of the cells was measured by enzyme immunoassay. *A*, S1P concentration-dependent inhibition of 1 μM forskolin-induced cAMP accumulation in the presence of 0.5 mM 3-isobutyl-1-methylxanthine. Forskolin-induced cAMP accumulation is expressed as 100%. *B*, MEF cells pretreated without and with PTX (100 ng/ml, 24 h) and then stimulated for 20 min with 1 μM S1P in the presence of 0.5 mM 3-isobutyl-1-methylxanthine. The effects of S1P were significant (*, $p < 0.01$). In all panels, data shown are the means ± S.E. of triplicate samples. *Error bars* are not shown when the bars are smaller than the size of the *data points*. *WT*, wild-type; *KO*, knockout.

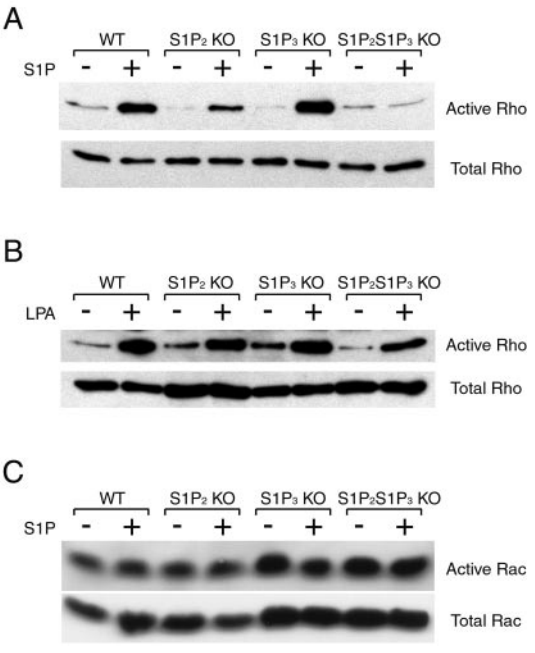

FIG. 6. **S1P-induced Rho activation in MEF cells.** Wild-type (*WT*) and knockout (*KO*) MEF cells were stimulated with 1 μM S1P (*A* and *C*) or LPA (*B*) for 3 min, and the cell lysate was used for affinity precipitation with Rhotekin Rho-binding domain- and PAK1 p21-binding domain-conjugated agarose beads to pull down activated forms of Rho and Rac, respectively. The lysate was also used to determine total Rho or Rac levels. Samples were separated on 15% SDS-polyacrylamide gels and analyzed by Western blot analysis using anti-RhoA or anti-Rac1 antibody. Data are representative of three independent experiments.

of this serum-borne bioactive lipid in the cardiovascular system. In fact, S1P$_1$-null mice were lethal between embryonic days 12.5 and 14.5 because of incomplete vascular maturation (8). Also, a single point mutation in the *s1p$_2$*-related *mil* gene in zebrafish leads to abnormal heart development (21). In contrast, S1P$_3$-null mice appear to be grossly normal (9). These results indicate that, despite similar expression patterns in mice, each receptor can have distinct roles.

The *s1p$_2$* gene was first isolated as a putative G protein-coupled receptor orphan from rat cardiovascular and nervous systems (22, 23). In the nervous system, *s1p$_2$* is preferentially expressed in young differentiating neuronal cell bodies and axons, and its temporal expression pattern is correlated with neuronal differentiation, including axon outgrowth (24). Moreover, experiments using antisense probes indicated that S1P$_2$ is involved in neurite outgrowth and cell to cell interactions

TABLE III
S1P cellular signaling properties in mutant MEF cells

S1P responses in wild-type cells are expressed as +++. + and ++ represent intermediate responses, and +/− and − stand for minimal and no responses, respectively. $[Ca^{2+}]_i$, intracellular $[Ca^{2+}]$; AC, adenylyl cyclase; KO, knockout.

	PLC activation	$[Ca^{2+}]_i$ increase	AC inhibition[a]	AC activation[b]	Rho activation
Wild-type	+++	+++	+++	+++	+++
$S1P_2$ KO	+++	+++	+++	++	+
$S1P_3$ KO	+	+/−	++	++	++
$S1P_2S1P_3$ KO	+	+/−	+++	−	−

[a] S1P-induced inhibition of forskolin-activated cAMP accumulation.
[b] S1P-induced cAMP accumulation observed with PTX-pretreated cells.

(25). These observations imply physiological roles of $S1P_2$ in nervous system development. To examine these hypothesized functions of $S1P_2$ *in vivo*, we generated $S1P_2$-null mice.

Our findings support nonessential roles of $S1P_2$ in normal mouse development. $S1P_2$-null mice were viable and fertile and developed normally, even though we observed slightly smaller litter sizes from homozygous-null mating ($s1p_2^{-/-} \times s1p_2^{-/-}$) (Table I), as seen with $S1P_3$-null mating (9). These data suggest a potential role of $S1P_2$ and $S1P_3$ in reproduction, as implied by expression of $s1p_2$ and $s1p_3$ in gonadal tissues (9), the abundant existence of S1P in testis (26), and prevention of oocyte apoptosis by S1P (27). However, functional and histological analyses revealed no obvious phenotypic abnormality in $S1P_2$-null reproductive and other organs examined. Previous studies on mammalian receptor overexpression systems showed that $S1P_2$ resembles $S1P_3$ in G protein coupling and signal transduction (28–32), even though a distinct role in Rac activation was recently reported in Chinese hamster ovary cells (33) and vascular smooth muscle cells (34). Our previous work demonstrated the possible compensatory expression of $s1p_2$ in $S1P_3$-null mouse brain and heart (9), which might explain the lack of major phenotypes in $S1P_3$-null mice. However, there was no such compensatory expression of *s1p* genes in $S1P_2$-null mice in this study (Fig. 1*D*, *left panel*).

In contrast to our findings, analyses of $S1P_2$-null mice in a recent study by MacLennan *et al*. (35) suggested more critical physiological role(s) of $S1P_2$ in mice. The authors observed that $S1P_2$-null mice occasionally had spontaneous and sporadic seizures between 3 and 7 weeks of age, accompanied by ictal-like electroencephalographic abnormalities and hyperexcitable neocortical pyramidal neurons with apparently normal structure of the nervous system (35). The seizures in $S1P_2$-null mice often (≅14%) resulted in death (35). We did not observe seizures or epileptic death in our $S1P_2$-null mice during those ages, and the basis for the discrepancy remains unclear. In our studies, almost all the pups (irrespective of genotypes) that survived through the first week after birth survived to adulthood. One possible explanation is a difference in the genetic background of the mutants: MacLennan *et al*. analyzed their mice on a C57BL/6 (albino) background (N2–N4), whereas we analyzed our mice on a C57BL/6N background (N3–N5).

The normal viability and fertility of $S1P_2$-null and $S1P_3$-null mice enabled us to generate $S1P_2S1P_3$ double-null mice. The deletion of both genes did not affect the expression of the other S1P receptor genes in the tissues tested (Fig. 1*D*, *right panel*). Double-null mice that survived were also viable and fertile and developed normally, similar to $S1P_2$-null and $S1P_3$-null mice. However, the numbers of double-null mice generated by various kinds of crossbreeding were fewer than expected (Table II). Most notably, double-null mice from double-null mating showed vastly reduced perinatal survival, which was not observed in other genetic crosses (Table II). The double-null matings produced only 65:21 = 3.1 pups/litter at birth, and only 1.2 pups/litter survived until weaning ages (n = 21) (Table II). Such low productivity and survival rates are not solely explainable by intrinsic defects in double-null pups because significant numbers of double-null mice could be generated from the other crosses (Table II). Similarly, the results cannot be solely accounted for by parental defects because $s1p_2^{-/-}s1p_3^{-/-}$ males × wild-type females as well as wild-type males × $s1p_2^{-/-}s1p_3^{-/-}$ females could produce and nurture significant numbers of pups (6.7 and 5.8 pups/litter, respectively). Thus, these data support an interpretation in which combined $S1P_2$ and $S1P_3$ receptor signaling has roles in prenatal development as well as parent-offspring interactions such as lactation and suckling. This latter interaction is reminiscent of the phenotype observed in mutants of the LPA_1 receptor (36), which is notable in view of the close evolutionary link between LPA and S1P receptors (4).

Clear alterations in S1P-induced signal transduction were observed in mutant MEF cells (summarized in Table III). The deletion of $s1p_2$ did not affect S1P-induced PLC activation on either the $s1p_3^{+/+}$ or $s1p_3^{-/-}$ background (Fig. 3), which supports our previous finding that $S1P_2$ is not involved in S1P-induced PLC activation in MEF cells (9). The deletion of $s1p_3$, but not $s1p_2$, diminished S1P-induced intracellular calcium mobilization (Fig. 4), indicating a primary role of $S1P_3$ in that response. The deletion of $s1p_2$ also did not affect S1P-induced inhibition of forskolin-activated cAMP accumulation (Fig. 5*A*). A slight decrease in sensitivity to S1P was observed in $S1P_3$-null MEF cells (Fig. 5*A*) (9), but not in $S1P_2S1P_3$ double-null MEF cells (Fig. 5*A*). In addition, S1P decreased basal cAMP production in a PTX-sensitive manner in $S1P_2S1P_3$ double-null MEFs. Because expression of $s1p_4$ and $s1p_5$ was not detectable in MEF cells (Fig. 2), these observations suggest a primary role of $S1P_1$ in S1P-induced adenylyl cyclase inhibition.

Previous studies using mammalian receptor overexpression systems indicated that $S1P_2$ and/or $S1P_3$ can mediate S1P-induced cAMP accumulation in the absence of forskolin, an adenylyl cyclase activator (Refs. 30 and 37; reviewed in Refs. 2 and 5). Using MEF cells, we have clearly shown that basal cAMP levels are regulated (or balanced) by two opposing S1P receptor-mediated signaling pathways. One is the PTX-sensitive, $G_{i/o}$-mediated adenylyl cyclase inhibition through $S1P_1$ described above. In addition, we observed PTX-insensitive adenylyl cyclase activation, which was observed when $G_{i/o}$ inhibition was blocked with PTX and which appeared to be mediated through $S1P_2$ and $S1P_3$ because it was lost in the double-null cells. These effects may be mediated via coupling to G_s or effects of elevated intracellular calcium or other adenylyl cyclase regulators such as protein kinase C (38, 39). Because $s1p_3$ overexpression enhances S1P inhibition of forskolin-activated cAMP accumulation in MEFs (9), the effect of $S1P_3$ on adenylyl cyclase activity may vary depending on the receptor expression levels or the activation state of adenylyl cyclase.

We previously showed that S1P induces Rho activation in wild-type MEF cells and that $S1P_3$ deletion does not affect this response (9). Because this S1P activation in wild-type MEFs is

PTX-insensitive (9) and the $S1P_1$ receptor has been shown to act only through PTX-sensitive G proteins, a prominent role of $S1P_2$ in S1P-induced Rho activation in MEF cells was postulated (9). In this study, we demonstrated that the deletion of $s1p_2$ resulted in a significant decrease in S1P-induced Rho activation, whereas responses to LPA remained intact (Fig. 6, *A* and *B*). Surprisingly, the S1P response was not fully lost in $S1P_2$-null MEF cells, although it was totally abolished in double-null MEF cells. The observation that the $s1p_3$ deletion did not significantly decrease S1P-induced Rho activation (Fig. 6) (9) may reflect the lack of sensitivity in quantifying small decreases in the amount of active Rho. However, it may also be argued that $S1P_2$ is the receptor that predominantly couples to the $G_{12/13}$/Rho pathway; only in its absence is the ability of $S1P_3$ to serve a redundant role in this fundamental response observed. S1P did not induce Rac activation in MEF cells, which contrasts with previous results by Liu *et al*. (8).

In this and previous (9) studies on single mutant mice, we demonstrated no requirement of $S1P_2$ or $S1P_3$ for normal development or physiological function of mice. Considering the universal expression of $s1p_{1-3}$ throughout the mouse body and the profound phenotypes found in $S1P_1$-null mice (*e.g.* hemorrhage and embryonic lethality), S1P-induced activation of PTX-sensitive G proteins ($G_{i/o}$) through $S1P_1$ rather than that of PTX-insensitive G proteins (G_q and $G_{12/13}$) through $S1P_2$ or $S1P_3$ seems to be essential for mouse development. Through $G_{i/o}$ proteins, S1P has been shown to activate mitogen-activated protein kinase and phosphoinositide 3-kinase (29, 40, 41), both of which are well characterized for their involvement in cell proliferation and survival, respectively. The defects in such $G_{i/o}$ downstream signaling could be relevant to the vascular phenotypes observed in $S1P_1$-null mice. However, S1P has also been shown to be a potent inducer of cell differentiation and migration responses, in which Rho activation by G_q or $G_{12/13}$ could play a major role (42, 43). In $S1P_2S1P_3$ double-null MEF cells, there was a complete loss of S1P-induced Rho activation, clearly showing non-redundant S1P signaling properties. In addition, greatly decreased litter size and marked perinatal lethality were observed in double-null mice. New phenotypes may be unmasked in these mutants when challenged by injury, disease, or other stressors.

Acknowledgments—We thank Grace Kennedy, Marisa Fontanoz, and Carol Akita for technical assistance.

REFERENCES

1. Spiegel, S., and Milstien, S. (2000) *Biochim. Biophys. Acta* **1484,** 107–116
2. Pyne, S., and Pyne, N. (2000) *Pharmacol. Ther.* **88,** 115–131
3. Pyne, S., and Pyne, N. J. (2000) *Biochem. J.* **349,** 385–402
4. Fukushima, N., Ishii, I., Contos, J. J., Weiner, J. A., and Chun, J. (2001) *Annu. Rev. Pharmacol. Toxicol.* **41,** 507–534
5. Takuwa, Y., Okamoto, H., Takuwa, N., Gonda, K., Sugimoto, N., and Sakurada, S. (2001) *Mol. Cell. Endocrinol.* **177,** 3–11
6. Tigyi, G. (2001) *Mol. Pharmacol.* **60,** 1161–1164
7. Hla, T., Lee, M. J., Ancellin, N., Paik, J. H., and Kluk, M. J. (2001) *Science* **294,** 1875–1878
8. Liu, Y., Wada, R., Yamashita, T., Mi, Y., Deng, C. X., Hobson, J. P., Rosenfeldt, H. M., Nava, V. E., Chae, S. S., Lee, M. J., Liu, C. H., Hla, T., Spiegel, S., and Proia, R. L. (2000) *J. Clin. Invest.* **106,** 951–961
9. Ishii, I., Friedman, B., Ye, X., Kawamura, S., McGiffert, C., Contos, J. J., Kingsbury, M. A., Zhang, G., Brown, J. H., and Chun, J. (2001) *J. Biol. Chem.* **276,** 33697–33704
10. Yagi, T., Nada, S., Watanabe, N., Tamemoto, H., Kohmura, N., Ikawa, Y., and Aizawa, S. (1993) *Anal. Biochem.* **214,** 77–86
11. Marth, J. D. (1996) *J. Clin. Invest.* **97,** 1999–2002
12. Zhang, G., Contos, J. J., Weiner, J. A., Fukushima, N., and Chun, J. (1999) *Gene* (*Amst.*) **227,** 89–99
13. Ishii, I., Contos, J. J., Fukushima, N., and Chun, J. (2000) *Mol. Pharmacol.* **58,** 895–902
14. Ishii, I., Izumi, T., Tsukamoto, H., Umeyama, H., Ui, M., and Shimizu, T. (1997) *J. Biol. Chem.* **272,** 7846–7854
15. Graler, M. H., Bernhardt, G., and Lipp, M. (1998) *Genomics* **53,** 164–169
16. Im, D. S., Heise, C. E., Ancellin, N., O'Dowd, B. F., Shei, G. J., Heavens, R. P., Rigby, M. R., Hla, T., Mandala, S., McAllister, G., George, S. R., and Lynch, K. R. (2000) *J. Biol. Chem.* **275,** 14281–14286
17. Liliom, K., Sun, G., Bunemann, M., Virag, T., Nusser, N., Baker, D. L., Wang, D. A., Fabian, M. J., Brandts, B., Bender, K., Eickel, A., Malik, K. U., Miller, D. D., Desiderio, D. M., Tigyi, G., and Pott, L. (2001) *Biochem. J.* **355,** 189–197
18. Tamama, K., Kon, J., Sato, K., Tomura, H., Kuwabara, A., Kimura, T., Kanda, T., Ohta, H., Ui, M., Kobayashi, I., and Okajima, F. (2001) *Biochem. J.* **353,** 139–146
19. Kimura, T., Watanabe, T., Sato, K., Kon, J., Tomura, H., Tamama, K., Kuwabara, A., Kanda, T., Kobayashi, I., Ohta, H., Ui, M., and Okajima, F. (2000) *Biochem. J.* **1,** 71–76
20. Wang, F., Van Brocklyn, J. R., Hobson, J. P., Movafagh, S., Zukowska-Grojec, Z., Milstien, S., and Spiegel, S. (1999) *J. Biol. Chem.* **274,** 35343–35350
21. Kupperman, E., An, S., Osborne, N., Waldron, S., and Stainier, D. Y. (2000) *Nature* **406,** 192–195
22. Okazaki, H., Ishizaka, N., Sakurai, T., Kurokawa, K., Goto, K., Kumada, M., and Takuwa, Y. (1993) *Biochem. Biophys. Res. Commun.* **190,** 1104–1109
23. MacLennan, A. J., Browe, C. S., Gaskin, A. A., Lado, D. C., and Shaw, G. (1994) *Mol. Cell. Neurosci.* **5,** 201–209
24. Maclennan, A. J., Marks, L., Gaskin, A. A., and Lee, N. (1997) *Neuroscience* **79,** 217–224
25. MacLennan, A. J., Devlin, B. K., Marks, L., Gaskin, A. A., Neitzel, K. L., and Lee, N. (2000) *Dev. Neurosci.* **22,** 283–295
26. Yatomi, Y., Igarashi, Y., Yang, L., Hisano, N., Qi, R., Asazuma, N., Satoh, K., Ozaki, Y., and Kume, S. (1997) *J. Biochem.* (*Tokyo*) **121,** 969–973
27. Morita, Y., Perez, G. I., Paris, F., Miranda, S. R., Ehleiter, D., Haimovitz-Friedman, A., Fuks, Z., Xie, Z., Reed, J. C., Schuchman, E. H., Kolesnick, R. N., and Tilly, J. L. (2000) *Nat. Med.* **6,** 1109–1114
28. Windh, R. T., Lee, M. J., Hla, T., An, S., Barr, A. J., and Manning, D. R. (1999) *J. Biol. Chem.* **274,** 27351–27358
29. An, S., Zheng, Y., and Bleu, T. (2000) *J. Biol. Chem.* **275,** 288–296
30. Kon, J., Sato, K., Watanabe, T., Tomura, H., Kuwabara, A., Kimura, T., Tamama, K., Ishizuka, T., Murata, N., Kanda, T., Kobayashi, I., Ohta, H., Ui, M., and Okajima, F. (1999) *J. Biol. Chem.* **274,** 23940–23947
31. Van Brocklyn, J. R., Tu, Z., Edsall, L. C., Schmidt, R. R., and Spiegel, S. (1999) *J. Biol. Chem.* **274,** 4626–4632
32. Ancellin, N., and Hla, T. (1999) *J. Biol. Chem.* **274,** 18997–19002
33. Okamoto, H., Takuwa, N., Yokomizo, T., Sugimoto, N., Sakurada, S., Shigematsu, H., and Takuwa, Y. (2000) *Mol. Cell. Biol.* **20,** 9247–9261
34. Ryu, Y., Takuwa, N., Sugimoto, N., Sakurada, S., Usui, S., Okamoto, H., Matsui, O., and Takuwa, Y. (2002) *Circ. Res.* **90,** 325–332
35. MacLennan, A. J., Carney, P. R., Zhu, W. J., Chaves, A. H., Garcia, J., Grimes, J. R., Anderson, K. J., Roper, S. N., and Lee, N. (2001) *Eur. J. Neurosci.* **14,** 203–209
36. Contos, J. J., Fukushima, N., Weiner, J. A., Kaushal, D., and Chun, J. (2000) *Proc. Natl. Acad. Sci. U. S. A.* **97,** 13384–13389
37. Gonda, K., Okamoto, H., Takuwa, N., Yatomi, Y., Okazaki, H., Sakurai, T., Kimura, S., Sillard, R., Harii, K., and Takuwa, Y. (1999) *Biochem. J.* **337,** 67–75
38. Taussig, R., and Gilman, A. G. (1995) *J. Biol. Chem.* **270,** 1–4
39. Hanoune, J., and Defer, N. (2001) *Annu. Rev. Pharmacol. Toxicol.* **41,** 145–174
40. Rakhit, S., Conway, A. M., Tate, R., Bower, T., Pyne, N. J., and Pyne, S. (1999) *Biochem. J.* **338,** 643–649
41. Banno, Y., Takuwa, Y., Akao, Y., Okamoto, H., Osawa, Y., Naganawa, T., Nakashima, S., Suh, P. G., and Nozawa, Y. (2001) *J. Biol. Chem.* **276,** 35622–35628
42. Lee, M. J., Thangada, S., Claffey, K. P., Ancellin, N., Liu, C. H., Kluk, M., Volpi, M., Sha'afi, R. I., and Hla, T. (1999) *Cell* **99,** 301–312
43. Paik, J. H., Chae, S., Lee, M. J., Thangada, S., and Hla, T. (2001) *J. Biol. Chem.* **276,** 11830–11837
44. Yang, A. H., Ishii, I., and Chun, J. (2002) *Biochim. Biophys. Acta*, in press